Synthetic phased-array terahertz imaging

John O'Hara and D. Grischkowsky

School of Electrical and Computer Engineering and Center for Laser and Photonics Research, Oklahoma State University, Stillwater, Oklahoma 74078

Received January 28, 2002

We demonstrate terahertz (THz) imaging with enhanced spatial resolution by a synthetic phased array. A single mirror is used to separately form two different coherent, diffraction-limited THz images of the same point source. The two images are combined to yield a 4× resolution-enhanced image of the source in one dimension. © 2002 Optical Society of America

OCIS codes: 110.5100, 250.0250, 320.0320.

For its great ability to increase resolution in imaging systems, aperture synthesis (AS) was a monumental concept. Radio astronomers began using AS in interferometers over 40 years ago[1] and continue today.[2,3] AS with independent optical telescopes began over 25 years ago[4] and has since[5] greatly improved ground-based optical astronomy. AS techniques enhance high-resolution radar[6,7] via deconvolution of many scattered fields. Terahertz (THz) images have been produced in the same fashion.[8] By diffraction theory, imaging has been done with numerical backpropagation of similar scattered THz fields.[9] THz reflection imaging with another inverse method, Kirchhoff migration, was recently demonstrated.[10] THz images have also been formed by scanning of a sample through a tightly focused THz beam, where either transmitted or reflected radiation is measured.[11,12] Electro-optic detection techniques have also been used to generate images without scanning the sample.[13]

We demonstrate THz imaging with phase-coherent, quasi-optic methods, where AS can be realized in a way very similar to modern, coherent, optical telescope arrays.[5] Unlike in radar[6–8] and scattered-field methods,[9,10] which use discrete measurements at various locations to realize AS and reconstruct an image, in the method presented here distinct optical mirrors are synthetically arrayed to form real, superposed images of THz illuminated objects. These images mutually interfere, yielding the benefit of AS without complex mathematical reconstruction. But, unlike optical telescopes,[4,5] which must simultaneously record images from each fixed array element, the THz system uses a phase-locked source, allowing images from each synthetically positioned element to be made independently and later combined. Moreover, because a sparse aperture arrangement is used, interferometric reconstruction is unnecessary. This approach is shown to increase dramatically the resolution of a quasi-optic THz imaging system.[14]

Image formation begins by illumination of an object with a THz beam consisting of a train of transform-limited, subpicosecond THz pulses[15] (which also provide ranging or timing information). A one-to-one, diffraction-limited image of the object is then projected in front of the fixed receiver, by the 152-mm-diameter spherical mirror, with a focal length of 305 mm, where the image is sampled and recorded as a set of time-dependent field measurements. The resolution of the system is defined by the size of the image of a point source. For increased resolution, two such images are formed separately and, by use of phased-array principles, combined coherently. The result is an image with enhanced resolution in one dimension. The object is a 1-mm-diameter steel sphere. Since only a small solid-angle portion of the sphere reflects radiation toward the mirror, the point-source approximation is valid and allows the one-to-one image to be smaller than 1 mm.

The quasi-optic THz imaging system in Fig. 1 is similar to that used in previous work,[14] with two major exceptions. First, the object can be moved in two dimensions, anywhere within the xy plane, to which the optic z axis is normal. Second, this plane of motion, or scan plane, can be rotated or tilted about the x axis. When the plane is tilted, 16° in our case, it is renamed the xy' plane so that the two configurations can be distinguished. The origin of the system is fixed in space and common to both configurations. Therefore the object lies in both planes simultaneously when it is on the x axis.

The resulting image data, $E_1(t, x, y)$ or $E_2(t, x, y')$, are sets of time-dependent field measurements for specific object locations in two-dimensional space.

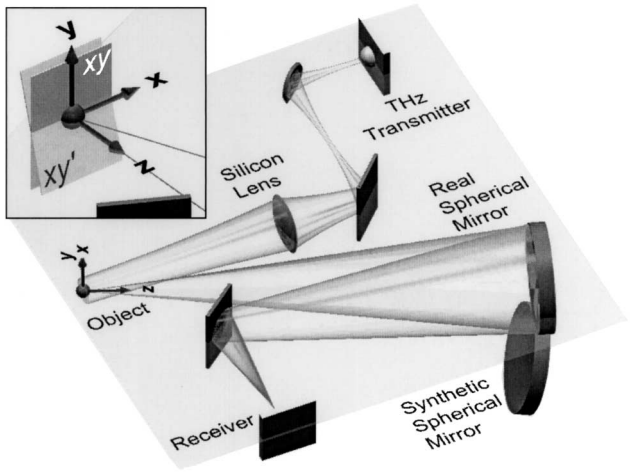

Fig. 1. Synthetic, phased-array THz system. The translucent cones show the THz beam. The lower spherical mirror is not physically in the setup. The inset shows a different view of the object and its planes of motion for the two configurations.

0146-9592/02/121070-03$15.00/0

The measurement $E_1(t, 0, 0)$ is shown in Fig. 2. The field amplitude is proportional to the measured current, and the time axis can be converted to distance, in z, so that the data can be considered a set of field measurements in three-dimensional space.

Conceptually, increasing the transverse resolution of the system is only a matter of increasing the size of the most-limiting aperture, defined here by the spherical mirror. Three methods to enlarge the aperture are to (1) use a larger mirror, (2) place another identical spherical mirror adjacent to the first and use phased-array principles, and (3) synthetically reproduce method (2) by use of the original mirror twice, each time with a different object orientation.

To implement method (3), we use the spherical mirror to make one image while the object scans in the normal configuration (xy plane). Then the spherical mirror is used to make the second image while the object is scanned in the tilted configuration (xy' plane). Scanning in the xy' plane forces the actual mirror to see the object from the viewpoint of the synthetic mirror and thereby generate the corresponding image. Figure 3 illustrates this situation.

When two coherent images are obtained, it becomes possible to synthesize a new image by simple addition of the two individual images in phase and amplitude. This composite image mimics the image that would be produced by the two-mirror system.

Even though the two images are recorded separately, they contain a measured phase relationship. The phase information contained in the time dependence of the electric field of the THz pulse is obtained with the very high sampling time resolution of 66 fs. Indeed, this explains the excellent z-direction (range) resolution of this imaging system, which is determined by the system bandwidth and its relative phase, not by diffraction. To establish its absolute phase, we center each image on the common origin by ensuring that the (0, 0, 0) position of the object for both configurations (tilted and normal) is the same point in three-dimensional space. In this way the individual image data overlap exactly (zero relative phase) when the object is at the origin. Since the phase relationship of the two images is highly dependent on the object placement in the z dimension, this placement is accurate to 15 μm, or less than 1/28 of a wavelength for 0.7 THz, the center of the spectrum. For the x and y (or y') dimensions, placement is within 120 μm, ~1/10 of a wavelength of the highest spatial frequency.

We now discuss the images shown in Fig. 4. First, consider the plane (henceforth called the xY plane) bisecting the two scan planes, xy and xy'. This xY plane represents the paraxial composite object plane of the two-mirror synthesized system. For plotting only, the variables y and y' may, to a good transverse approximation, be treated as the same variable Y (i.e., $y = y' = Y$). Second, since we wish to present the transverse spatial (x, Y) profile of the image, it is essential to have time-independent methods of plotting the images.

One such method is to plot the images in terms of energy $U(x, Y)$, where

$$U(x, Y) = \int (E_1 + E_2)^2 \mathrm{d}t = \int (E_1{}^2 + E_2{}^2 + 2E_1E_2)\mathrm{d}t\,, \quad (1)$$

which is then defined term by term as

$$U(x, Y) \equiv U_1(x, Y) + U_2(x, Y) + U_{12}(x, Y)\,. \quad (2)$$

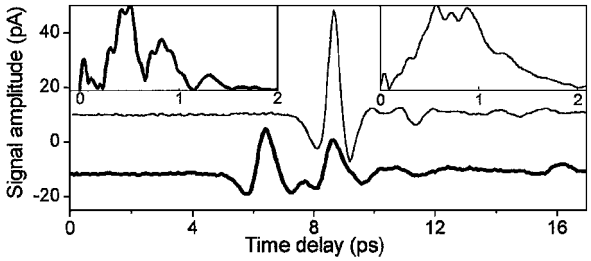

Fig. 2. Top, light curve, measurement $E_1(t, 0, 0)$, offset +10 pA; bottom, heavy curve; superposition, $E_1(t, 0, 1.375\ \mathrm{mm}) + E_2(t, 0, 1.375\ \mathrm{mm})$, offset −12 pA. The right and left insets are their respective normalized spectra in THz. The peak signal-to-noise ratio for E_1 and E_2 is ~200:1.

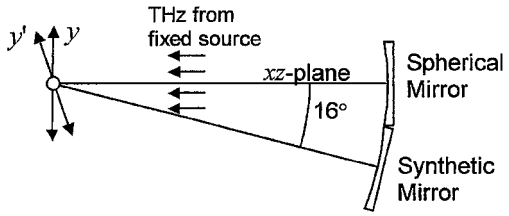

Fig. 3. Side view of the THz imaging system showing the location of the synthetic mirror. The synthetic mirror's viewpoint of the object being scanned in the xy plane is the same as the actual mirror's viewpoint of the object being scanned in the xy' plane.

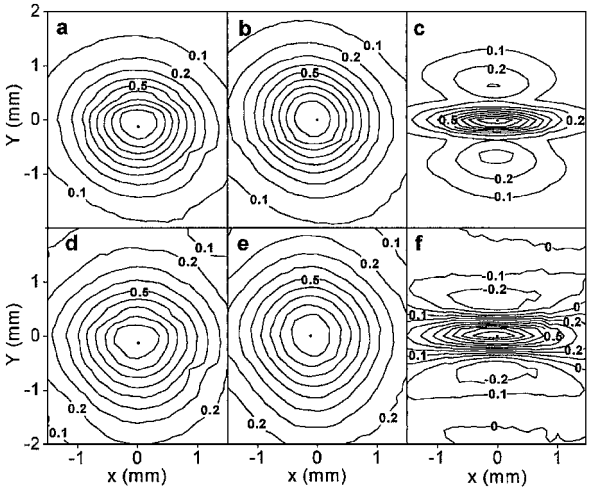

Fig. 4. Normalized images of a THz point source. a, b, Individual energy images U_1 and U_2, respectively. c, Composite energy image from the synthetic two-mirror system. d, e, Field images E_1 and E_2, respectively. f, Synthetic two-mirror field image in the composite image plane with positive and negative values. The contour separation is 0.1.

E_1 and E_2 are the individual image data from the normal and tilted configurations, respectively, and $E_1 + E_2$ is their coherent superposition. $U_1(x, Y)$ and $U_2(x, Y)$ therefore describe the individual energy images shown in Figs. 4a and 4b, respectively. $U(x, Y)$ represents the composite energy image shown in Fig. 4c. If one had THz photographic film or a THz CCD camera to capture the two-mirror image, $U(x, Y)$ would be the image obtained.

Since the THz system measures the time-dependent electric field, it is desirable to display the images showing the coherent superposition of the field amplitudes. One such method is to plot the peak field amplitude of E_1 and E_2 for each (x, Y) point, as in Figs. 4d and 4e. Plotting the single peak (see Fig. 2) of each scan is meaningful because this temporal point represents the location of constructive phase coherence for all the THz components.[15] Figures 4d and 4e show the FWHM of the image (the 0.5 contour) to be ~2.0 mm, consistent with theory and previous work.[14]

The relative time shifts between scans of the composite image $(E_1 + E_2)$ define the phase relationship of the two images. So, for the superposition data, shown in Fig. 4f, the field amplitude is plotted at the time midway between the pulses in the scans that constitute E_1 and E_2 (see Fig. 2). This procedure reveals the maximum coherent overlap between the two individual images and displays the combined electric field image in the paraxial composite image plane corresponding to the composite object plane (the xY plane).

To understand this, consider that the superposition data at (x, Y) consist of two similar electric field pulses, whose separation in time, to first order, is proportional to the product of Y and the angle between the xy and xy' planes. Therefore, these pulses will have a maximum time separation at the far ends of the Y scans. On one end, the E_1 pulse will occur earlier than the E_2 pulse. The opposite is true for the other end of the Y scan. The two pulses smoothly pass through each other as a function of Y during the scan and overlap precisely at the $(x = 0, Y = 0)$ position. The interference between E_1 and E_2 is greatest at the time halfway between the two pulses.

The effects of the phased-array system are obvious in Figs. 4c and 4f. In the vertical Y dimension, the width of the image is reduced and two sidelobes appear, whereas no significant change is apparent in the horizontal x dimension. This was expected since the synthetic mirror increased the effective aperture size in the vertical dimension only. As in any arrayed system, the sidelobes appear as a consequence of the sparse composite aperture. Both the magnitude and the position of the sidelobes in Figs. 4c and 4f agree to within 10% of our calculated values.

Surprisingly, Figs. 4c and 4f show that the decrease in width (or increase in resolution) of the image was approximately four times in the Y dimension, instead of the expected two times. This discrepancy is a consequence of the fact that both configurations have the same fixed THz illumination source. In the tilted configuration additional phase changes are introduced as the object changes distance from the source (in $\pm z$ directions) when it is scanned in the $\mp y'$ directions. This phase causes a larger apparent mirror separation and synthetic aperture. To our advantage, the larger separation and aperture correspondingly increase resolution, which is directly related to observed phase differences. For a self-luminous object, this effect would not occur. Since this system is linear for small, close objects, two point sources separated vertically by as little as 0.4 mm could be spatially resolvable. This value represents the Rayleigh resolution criterion wherein the center of the image of one object lies directly over the first zero crossing of the image of the other object. As with previous work,[14] the two objects would be even more resolvable in the temporal z direction.

In summary, we have demonstrated the first quasi-optic aperture synthesis imaging done with real THz images. In our AS technique, we have, for what is believed to be the first time at any frequency, recorded coherent field images of the individual elements of a coherent array. These two images were later combined to form the image of the complete array. By extension of this technique to more elements, this AS method should produce images with resolution comparable to the wavelength employed.

This research was partially supported by the National Science Foundation and the U.S. Army Research Office. D. Grischkowsky's e-mail address is grischd@ceat.okstate.edu.

References

1. M. Ryle and A. Hewish, Mon. Not. R. Astron. Soc. **120,** 220 (1960).
2. P. J. Napier, A. R. Thompson, and R. D. Ekers, Proc. IEEE **71,** 1295 (1983).
3. P. J. Napier, D. S. Bagri, B. G. Clark, A. E. E. Rogers, J. D. Romney, A. R. Thompson, and R. C. Walker, Proc. IEEE **82,** 658 (1994).
4. A. Labeyrie, Astrophys. J. **196,** L71 (1975).
5. A. R. Hajian and J. T. Armstrong, Sci. Am. **284,** 56 (2001).
6. D. Mensa, *High Resolution Radar Imaging* (Artech House, Norwood, Mass., 1981).
7. A. Broquetas, J. Palau, L. Jofre, and A. Cardama, IEEE Trans. Antennas Propag. **46,** 730 (1998).
8. K. McClatchey, M. T. Reiten, and R. A. Cheville, Appl. Phys. Lett. **79,** 4485 (2001).
9. A. B. Ruffin, J. Decker, L. Sanchez-Palencia, L. Le Hors, J. F. Whitaker, T. B. Norris, and J. V. Rudd, Opt. Lett. **26,** 681 (2001).
10. T. D. Dorney, J. L. Johnson, J. Van Rudd, R. G. Baraniuk, W. W. Symes, and D. M. Mittleman, Opt. Lett. **26,** 1513 (2001).
11. B. B. Hu and M. C. Nuss, Opt. Lett. **20,** 1716 (1995).
12. D. M. Mittleman, M. Gupta, R. Neelamani, R. G. Baraniuk, J. V. Rudd, and M. Koch, Appl. Phys. B **68,** 1085 (1999).
13. Q. Wu, T. D. Hewitt, and X.-C. Zhang, Opt. Lett. **69,** 1026 (1996).
14. J. O'Hara and D. Grischkowsky, Opt. Lett. **26,** 1918 (2001).
15. M. van Exter and D. Grischkowsky, IEEE Trans. Microwave Theory Technol. **38,** 1684 (1990).